Resonant Ion-Dip Infrared Spectroscopy of Ternary Benzene−(Water)$_n$(Methanol)$_m$ Hydrogen-Bonded Clusters

Christopher J. Gruenloh, Fredrick C. Hagemeister, Joel R. Carney, and Timothy S. Zwier*

Department of Chemistry, Purdue University, West Lafayette, Indiana 47907-1393

Received: September 3, 1998; In Final Form: November 13, 1998

Resonant two-photon ionization, IR−UV hole-burning, and resonant ion-dip infrared (RIDIR) spectroscopies have been employed along with density functional theory (DFT) calculations to assign and characterize the hydrogen-bonded topologies and structures of eight benzene−$(H_2O)_n(CH_3OH)_m$, cluster isomers (hereafter shortened to BW_nM_m) with $n + m \leq 4$. The O−H stretch infrared fundamentals are used to determine the H-bonding topology of the clusters. However, in several cases, the O−H stretch spectrum leaves an ambiguity regarding the position of the methanols within the structure. In these cases, the methyl CH stretch region serves as a secondary probe capable of distinguishing among the various possibilities. For $n + m = 2$, a single BWM isomer is observed with OH stretch fundamentals at 3508, 3606, and 3718 cm^{-1}. A comparison of the methyl CH stretch transitions of BWM and BM_2 reveals that the methanol in BWM accepts a H-bond from water and forms a π H-bond with benzene. The $n + m = 3$ results show the subtle effects that solvent composition can have on the lowest-energy structure of the cluster. Two isomers of BW_2M are observed but just one of BWM_2. Both water-rich BW_2M isomers possess transitions characteristic of *cyclic* W_2M subclusters in which water is π H-bonded to benzene. Each isomer shows a set of three single-donor OH stretch transitions, a π H-bonded OH stretch near 3650 cm^{-1} and a free OH stretch ($\sim$3716 cm^{-1}). The two BW_2M isomers differ in the position of the methanol in the H-bonded cycles. Conversely, the methanol-rich BWM_2 cluster OH stretch transitions are those of a WM_2 *chain*, with a signature π H-bonded OH stretch located at about 3590 cm^{-1}. The methyl CH stretch absorptions are used to deduce that the water molecule in BWM_2 is in the donor position in the chain, furthest from benzene's π cloud. Finally, the spectra for the $n + m = 4$ series show systematic changes in the spectrum with changing methanol content in the cluster. In all cases, both OH stretch and CH stretch transitions point firmly to *cyclic* W_nM_m subclusters in which one of the free OH groups on a water molecule in the cycle is used to π H-bond to benzene.

I. Introduction

One of the useful parameters available to the practicing chemist who seeks to increase the solubility of a reagent or alter its reactivity is the solvent composition.[1−3] Water/alcohol mixtures play a particularly important role as polar solvents.[1−4] The two liquids are completely miscible in one another, enabling fine-tuning of the solvent composition over a wide range. At the same time, the length and shape of the alkyl chain of the alcohol provide an easy means of modifying the ability of the solution to dissolve nonpolar compounds.

Recent progress has been made in describing the composition of bulk alcohol/water mixtures using techniques such as IR,[5−7] Raman,[5,8−10] Rayleigh scattering,[11] neutron and X-ray diffraction,[12,13] NMR,[14] microwave dielectric analysis,[15] mass spectrometry,[16] and HPLC.[17] Analysis of these data is often carried out by assuming that the binary liquid mixture is composed of a few key cluster structures that dominate the liquid. However, firm insight to the local environments of mixed-solvent solutions is difficult by such methods, which simultaneously sample all local environments present in the bulk mixture.

For this reason, the study of gas-phase clusters of water and alcohol provides a unique venue for studying solvation effects. In favorable cases, the spectroscopic consequences of a single solvent structure can be studied free from interference from others present in the expansion. Recently, tremendous progress has been made in understanding the structures and cooperative strengthening present in H-bonded networks found in pure water[18] and pure methanol[19−22] clusters. These studies serve as benchmarks against which mixed-solvent cluster data can be compared, but due to experimental difficulties in selectively probing mixed water−methanol clusters, results have thus far has been limited to the water−methanol dimer.[23−26]

When the study of binary solvent mixtures is expanded to include a third component (e.g., a solute such as benzene), issues of preferential solvation[27] arise, in which the local solvent composition about a solute may differ from that of the bulk mixture. In this context, the preferential solvation of benzene by water or methanol molecules is interesting, since both benzene and water are highly soluble in methanol but immiscible with one another;[28] therefore, studies of their clusters have the potential to probe the structural consequences of this disruption on a molecular scale.

In the present study of benzene−$(H_2O)_n(CH_3OH)_m$ clusters (denoted BW_nM_m), we seek to spectroscopically characterize the lowest-energy BW_nM_m cluster structures, thereby bridging between the pure BW_n and BM_m clusters studied previously. One can anticipate that the study of ternary gas-phase clusters will present a special experimental challenge. As illustrated in Figure 1 for the BW_2M cluster, clusters of the same composition could in principle take up differing H-bonding topologies (e.g., cycles as in (a) and (b) of Figure 1 vs chains as in (c) and (d)), differing positions of methanol substitution in the same H-

10.1021/jp983630k CCC: $18.00
Published on Web 01/09/1999

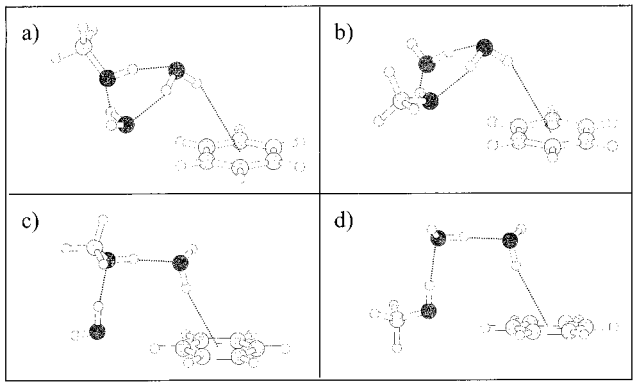

Figure 1. BW_2M structures illustrating the types of isomers that can arise in a three-component cluster such as this. Structural isomers can exist that differ in the H-bonding topology of the cluster (cycles (a, b) vs chains (c, d)), the position of methanol substitution in a given H-bonding topology (c vs d), and different points of attachment of the W_2M cluster to benzene (a vs b).

bonding structure (e.g., Figure 1c vs 1d), and/or different positions of attachment of benzene to a given W_nM_m cluster (Figure 1a vs 1b.

The present paper builds on our earlier resonant two-photon ionization (R2PI) study[29] of BW_nM_m clusters with $n + m \leq 4$. In that work, several of the main features of the cluster structures were deduced using a battery of vibronic level probes. Specifically, the W_nM_m subclusters impose perturbations on the ultraviolet chromophore benzene which (i) produce $S_1 \leftarrow S_0$ electronic frequency shifts, (ii) induce intensity in the otherwise electric dipole forbidden $S_1 \leftarrow S_0$ origin, (iii) split the degeneracy of the $v_6 = 1$ level in the S_1 state, and (iv) produce intermolecular vibrational structure which together provided clues to the H-bonding topology of the W_nM_m clusters. Here we extend the previous work by employing resonant ion-dip infrared spectroscopy (RIDIRS) to characterize the clusters.[30−35] The combined tools of R2PI and RIDIRS enable us to identify two new conformational isomers in the $n + m \leq 4$ clusters. The RIDIRS scans in the OH stretch region provide a much more direct and unambiguous probe of the H-bonding topology of the BW_nM_m clusters. As an aid in assigning the H-bonded topologies and substitutional isomers of these mixed clusters, comparisons will be made to previous RIDIRS studies of BW_n[30−33] and BM_m[34,35] and to calculated vibrational frequencies and infrared intensities of several of the most stable BW_nM_m structures. In two cases, the position of the methanol molecule(s) in the cluster is not unambiguously assigned by the OH stretch spectrum. Here, the methyl CH stretch spectrum is used as a secondary probe to resolve the issue.

II. Methods

The experimental methods and conditions used in the present work are essentially the same as those used for the BM_m clusters.[36] Typical sample concentrations in the expansion are 0.2−0.4% benzene, 0.2−0.3% water, and 0.1−0.2% methanol in a balance of Ne-70 at a total pressure of 2 bar.

One-color R2PI spectra are collected by gating around the arrival times of $BW_nM_m^+$ clusters and recording the ion intensity present in those gates as a function of laser wavelength, using a digital oscilloscope interfaced to a personal computer. RIDIR spectra of the clusters in the OH and CH stretch regions are recorded using the 6_0^1 transitions of the BW_nM_m clusters as intermediate states in the R2PI detection step.

The double resonance technique of IR−UV hole-burning spectroscopy[37] is used to determine the number of ground-state species contributing to the R2PI spectrum in the BM^+ mass channel. This pump−probe method employs the IR output of a Nd:YAG-pumped optical parametric oscillator (OPO) to remove a significant fraction of the population from a selected ground state by exciting a specified OH stretch mode. Then, a UV laser is tuned through the R2PI spectrum, and the difference in ion signals with and without the hole-burning laser present is recorded. Transitions sharing the same initial state as that probed by the IR hole-burning laser are detected as dips in the ion signal.

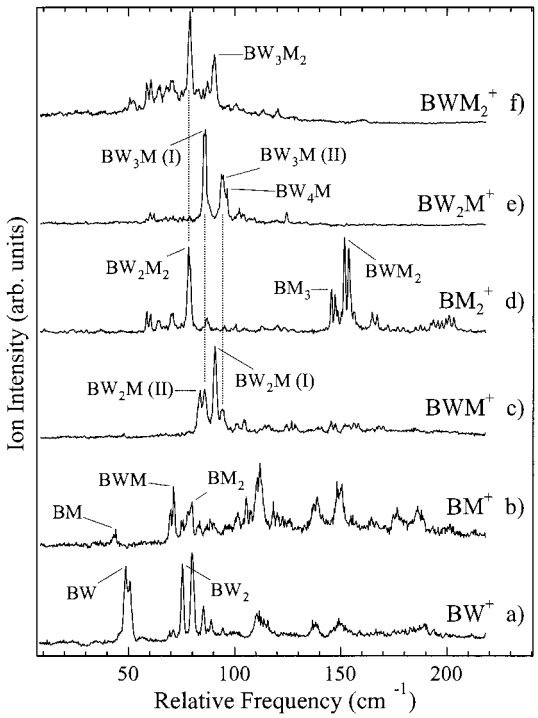

Figure 2. One-color R2PI spectra recorded in the 6_0^1 region of the $S_1 \leftarrow S_0$ transition of benzene, monitoring the $BW_nM_m^+$ mass channels with (a) and (b) $n + m = 1$, (c) and (d) $n + m = 2$, and (d)−(g) $n + m = 3$. The zero of the frequency scale corresponds to the 6_0^1 transition of the benzene monomer (38 609 cm^{-1}). Note that clusters undergo ionization-induced fragmentation with $BW_{n-1}M_m^+$ as the primary fragment channel. The transitions and mass channels used to record RIDIR spectra of the clusters are labeled in the spectra.

Structures, binding energies, harmonic vibrational frequencies, and infrared intensities have been computed for representative BW_nM_m structural types to compare with experiment. As in our previous work on M_m and BM_m clusters,[34,35] density functional theory (DFT) was employed using the Becke3LYP functional with a 6-31+G(d) basis set.[38−43] This level of theory obtains structures and OH stretch vibrational frequency shifts for $(water)_n$, benzene−$(water)_n$,[33,44−46] and benzene−$(methanol)_m$ clusters[34,35] that are in close correspondence with the results of both experiment and MP2 (second-order Moller−Plesset) calculations employing similar basis sets.

III. Results and Analysis

A. R2PI and IR−UV Hole-Burning Spectra. One-color R2PI spectra of BW_nM_m clusters are presented in Figure 2, recorded near the 6_0^1 region of the $S_1 \leftarrow S_0$ transition of benzene by monitoring the $BW_nM_m^+$ mass channels with $n + m = 1-3$. The R2PI transitions are plotted as frequency shifts with respect to the vibronically allowed 6_0^1 $S_1 \leftarrow S_0$ transition of benzene (38 609 cm^{-1}). These spectra differ from those reported earlier[29] by virtue of the more efficient cooling obtained

TABLE 1: One-Color Resonant Two-Photon Ionization Transitions of BW_nM_m Clusters

$n + m$	frequency shift[a] (cm^{-1})	mass fragment channel(s)[b]	cluster assignment
2	75[c]	BW	BW_2
	71[d]	BM, BW	BWM
	80[e]	BM	BM_2
3	98[c]	BW_2	BW_3
	91[d]	BWM	BW_2M(I)
	84	BWM	BW_2M(II)
	154[d]	BM_2, BWM	BWM_2
	147[e]	BM_2	BM_3
4	100[c]	BW_3	BW_4
	94	BW_2M, BWM	BW_3M(II)
	86[d]	BW_2M, BWM	BW_3M(I)
	79[d]	BM_2, BWM_2	BW_2M_2
	64[d]	BM_3	BWM_3
	19[e]	BM_3	BM_4

[a] Frequency shift relative to the 6_0^1 transition of the benzene monomer (38 609 cm^{-1}). [b] Neutral clusters fragment following photoionization and are detected in these mass channels. [c] Assigned in refs 47 and 48. [d] Assigned in ref 29. [e] Assigned in ref 49.

in the current work using Ne-70 as carrier gas rather than helium. This improved cooling removes much of the broad background that complicated prior work and enables the resolution and identification of several new transitions attributable to mixed BW_nM_m clusters. Table 1 lists 6_0^1 frequency shifts, photoionization-induced fragment channels, and cluster assignments as a function of the number of solvent molecules for BW_n,[47,48] BW_nM_m,[29] and BM_m[49] clusters with $n + m = 2-4$. Benzene concentration studies (not shown), performed to identify sources of interference due to $B_xW_nM_m$ ($x = 2$, 3, etc.) clusters, indicated no contribution from these larger clusters in the mass channels of Figure 2. Data from earlier reports on BW_n and BM_m clusters has been included throughout this paper to highlight the change in the UV and IR spectra of the clusters in going from pure benzene−water clusters to pure benzene−methanol clusters.

One issue complicating the study of benzene/hydrogen-bonded solvent clusters is that fragmentation by evaporative loss of solvent monomers following resonant photoionization can occur if sufficient internal energy is given to the cluster during photoionization.[29,48,50] In cases where the lowest energy structure for the ionized cluster is very different from that of the neutral cluster, Franck−Condon factors will favor ion geometries well above the adiabatic ionization threshold where fragmentation is possible. Our previous R2PI study[29] of BW_nM_m mixed clusters showed that these clusters fragment preferentially by loss of water monomers over methanol following one-color photoionization, and accordingly, the BW_nM_m R2PI spectra are collected in the $BW_{n-1}M_m^+$ and $BW_{n-2}M_m^+$ mass channels. Small clusters ($n + m \leq 3$) fragment by losing a single water molecule and are detected only in the $BW_{n-1}M_m^+$ mass channel. The loss of a second water molecule becomes energetically allowed in the $n + m = 4$ mixed clusters, and these are detected in both the $BW_{n-1}M_m^+$ and $BW_{n-2}M_m^+$ mass channels.

In our previous study, R2PI transitions assigned to the dominant isomers of the BW_nM_m clusters with $n + m \leq 4$ were assigned and analyzed.[29] In the present work, improvements in the R2PI spectra and the additional information provided by RIDIR spectroscopy has provided the assignment of two additional isomers with $n + m \leq 4$.

1. BWM Cluster. The ultraviolet transitions assigned to the BWM cluster appear in the BM^+ mass channel and are found amidst those due to BM_2 (Figure 3b,c). Unlike the larger clusters, which show little Franck−Condon activity in intermolecular vibrations, both BWM and BM_2 show extensive and intense intermolecular combination bands that are heavily overlapped with one another. To extricate the BWM R2PI spectrum from that due to BM_2, IR−UV hole-burning experiments were carried out. The hole-burning spectrum of Figure 3a was obtained with the IR OPO used for hole-burning fixed on the free OH stretch fundamental of BWM at 3718 cm^{-1} (assigned in the next section). As expected, the hole-burning spectrum reveals extensive intermolecular structure for BWM, much like that in BM_2. The spectrum of Figure 3a also confirms that the 6_0^1 transition of BWM is not overlapped with BM_2, enabling us to record the RIDIR spectrum of BWM without interference from the BM_2 cluster. Furthermore, the fact that all structure in the R2PI spectrum of Figure 3b can be accounted for as the sum of Figure 3a,c gives evidence that a single BWM isomer is responsible for all structure observed.

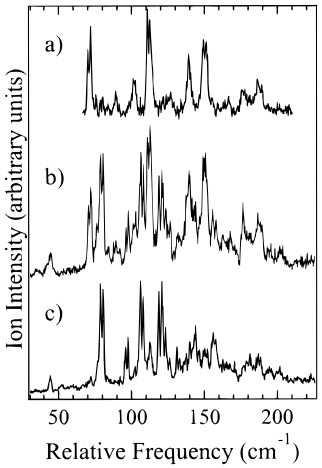

Figure 3. (a) IR−UV hole-burning spectrum of transitions assigned to BWM in the BM^+ mass channel with ν_{IR} fixed at 3718 cm^{-1}, the free OH stretch of BWM. (b) One-color R2PI spectrum monitoring the BM^+ mass with water, methanol, and benzene present in the supersonic expansion. Transitions due to both BWM and BM_2 are present. (c) One-color R2PI spectrum monitoring BM^+ with only methanol and benzene present. The transitions beginning at +80 cm^{-1} are due to BM_2. The zero of the frequency scale corresponds to the 6_0^1 transition of the benzene monomer (38 609 cm^{-1}). Transitions due to the BM_2 and BWM clusters were detected in the BM^+ mass channel after ionization-induced fragmentation of one methanol or water molecule, respectively.

2. BW_nM_m Isomers with $n + m = 3, 4$. In the present study, a new R2PI transition was found (Figure 2c) in the BWM^+ mass channel with a frequency shift of +84 cm^{-1}, just 7 cm^{-1} away from the dominant transition assigned to BW_2M in earlier work (+91 cm^{-1}).[29] If the cluster follows a fragmentation pattern similar to those of other BW_nM_m clusters, its presence exclusively in this mass channel points to an assignment as a second structural isomer of BW_2M. Its close proximity to BW_2M(I) points to a similar interaction of the W_2M(II) and W_2M(I) subclusters with benzene. In our earlier R2PI study,[29] the BW_2M(I) isomer was tentatively assigned to a cyclic W_2M isomer π H-bonded to benzene. A similar structure for BW_2M(II) is thereby suggested by the R2PI spectrum, but this will need to be tested by RIDIRS.

Similarly, the +94 cm^{-1} transition present in the BW_2M^+ and BWM^+ mass channels is assigned to a second isomer of the BW_3M cluster, also not identified in previous work. Again, the frequency shift (+94 cm^{-1}) is close to those of the cyclic BW_4 and BW_3M(I) clusters at +100 and +86 cm^{-1}, respectively, suggesting that BW_3M(II) is a second, cyclic isomer of BW_3M.

TABLE 2: Key Structural Parameters for Selected W_nM_m and BW_nM_m Theoretical Structures Studied Herein[a]

cluster	OH type[b]	R(OH) (Å)	$R(\pi$Acc)[c] (Å)	A(OHO)[d] (deg)	A(OOO)[e] (deg)	cluster	OH type[b]	R(OH) (Å)	$R(\pi$Acc)[c] (Å)	A(OHO)[d] (deg)	A(OOO)[e] (deg)
WM (A)	free OH	0.97				BW_2M (B)	πOH	0.971	4.022		
	S	0.979	2.852	172.43			S	0.982	2.811	147.74	59.35
WM (B)	free OH	0.97					S	0.986	2.760	149.81	59.47
	S	0.976	2.882	174.186			S	0.985	2.764	152.31	61.18
BW_2	πOH	0.975	3.859			M_3 (chain)	free OH	0.968			
	S	0.980	2.842	163.65			S	0.982	2.794	167.56	
							S	0.983	2.799	166.64	85.15
BWM (A)	πOH	0.974	3.892								
	S	0.981	2.827	164.81		WM_2 (A)	S (M)	0.984	2.766	151.20	60.66
BWM (B)	πOH	0.974	3.857				S (W)	0.986	2.753	151.19	59.91
	S	0.978	2.852	165.68			S (M)	0.982	2.787	147.75	59.43
BM_2	πOH	0.973	3.880			BM_3	πOH	0.975	3.734		
	S	0.980	2.838	166.97			S	0.985	2.782	173.60	95.25
							S	0.984	2.795	171.84	
W_3	S	0.985	2.767	150.09	59.90						
	S	0.985	2.766	150.19	60.21	BWM_2 (A)	πOH	0.975	3.738		
	S	0.984	2.776	147.42	59.89		S	0.985	2.781	173.25	95.22
							S	0.986	2.787	170.60	
BW_3	πOH	0.971	4.053								
	S	0.982	2.815	147.52	59.72	BWM_2 (B)	πOH	0.975	3.737		
	S	0.984	2.772	147.68	58.98		S	0.987	2.771	173.92	97.25
	S	0.988	2.751	152.47	61.30		S	0.983	2.805	171.84	
BW_2M (A)	πOH	0.971	4.052			BWM_2 (C)	πOH	0.976	3.699		
	S	0.984	2.800	149.50	60.28		S	0.983	2.797	172.40	94.48
	S	0.982	2.788	148.27	58.99		S	0.984	2.797	171.70	
	S	0.988	2.751	152.16	60.72						

[a] Calculated at the Becke3LYP/6-31+G(d) level of theory. [b] The OH subunits are ordered by first including the π-donor OH and then all single-donor OH's following the chain of hydrogen bonds from the π-donor. [c] The reported distance is from oxygen on the OH subunit to its HB acceptor. In the case of the π-HB, the distance is to the center of the benzene ring. [d] The OHO angle is for the HB that includes the OH subunit. [e] The OOO angle includes the oxygen atom from the OH subunit acting as the vertex and the oxygen atoms from nearest neighbor OH subunits.

B. Density Functional Theory Calculations. An extensive set of DFT Becke3LYP/6-31+G(d) calculations on W_nM_m and BW_nM_m clusters with $n + m = 2-4$ were carried out. The primary goal of this computational work was to use the calculated vibrational frequencies as an aid in assigning the carrier of a given RIDIR spectrum to a specific cluster species. The predicted structures and binding energies can also provide a point of comparison with other calculations on the mixed W_nM_m clusters, which are just beginning to be studied by high-level theory.[51] Beyond this, the DFT results on the W_nM_m clusters are predictions that can aid future experimental searches for these clusters, which have thus far gone undetected.

The key structural parameters computed for the W_nM_m and BW_nM_m clusters with $n + m = 2-4$ are collected in Table 2. The computed binding energies of these clusters, both with and without zero-point energy corrections, are given in Table 3. Finally, Table 4 presents the computed OH stretch harmonic vibrational frequencies and infrared intensities for the BW_nM_m clusters with $n + m = 2$ and 3.[52]

C. RIDIR Spectra and the Comparison with Theory. Overview RIDIR spectra of the BW_nM_m series with $n + m = 2-4$ in the OH and CH stretch regions of the infrared are shown in Figures 4−6, respectively. The frequencies, frequency shifts, widths, and assignments for OH stretch vibrations of a given cluster are listed in Table 5. The RIDIR spectrum for each cluster was obtained by monitoring the ion signal that results from fixing the R2PI laser on that particular cluster's 6_0^1 transition, shown as labeled transitions in Figure 2. The RIDIR spectra of Figures 4−6 consist of hydride stretch transitions that can be grouped into one of five characteristic types: (i) free OH stretches appearing near 3715 cm^{-1}, (ii) the C_6H_6/H_2O (W→B, hereafter) or C_6H_6/MeOH (M→B, hereafter) π H-bonded OH stretches that appear between 3590 and 3660 cm^{-1}, (iii) the single-donor O−H···O stretch fundamentals in the 3100−3500 cm^{-1} region, (iv) the sharp, Fermi resonance-coupled CH stretches of benzene between 3040 and 3100 cm^{-1}, and (v) the CH stretches of the methyl groups in the 2800−3000 cm^{-1} region.

TABLE 3: DFT Calculated Energies for W_nM_m and BW_nM_m Clusters[a]

cluster	H-bonded topolgy	binding energies: uncorrected	binding energies: ZPE corrected[b]	relative energy[c]
WM (A)	chain	−6.68	−4.49	0.00
WM (B)	chain	−6.19	−4.27	0.22
BWM (A)	chain	−10.34	−7.33	0.00
BWM (B)	chain	−9.88	−7.00	0.33
WM_2 (A)	cycle	−18.91	−14.25	0.00
WM_2 (B)	chain	−15.31	−11.3	2.95
BWM_2 (A)	chain	−20.20	−15.48	0.35
BWM_2 (B)	chain	−20.04	−15.21	0.61
BWM_2 (C)	chain	−19.71	−15.12	0.71
BWM_2 (D)	cycle	−21.04	−15.82	0.00
W_2M (A)	cycle	−19.21	−13.78	0.00
W_2M (B)	cycle	−19.16	−13.76	0.02
W_2M (C)	cycle	−19.16	−13.69	0.09
W_2M (D)	cycle	−18.04	−13.11	0.67
BW_2M (A)	cycle	−21.45	−15.44	0.00
BW_2M (B)	cycle	−21.45	−15.38	0.06
BW_2M (C)	chain	−20.45	*d*	*d*

[a] Calculations performed at the Becke3LYP/6-31+G(d) level of theory. All energies reported in kcal/mol. [b] Zero-point energy corrections from frequency calculations at the same level of theory. [c] Relative energy with respect to the lowest energy (ZPE-corrected) structure. [d] Frequency calculations were not performed at this high-energy structure.

1. BW_nM_m with $n + m = 2$. The RIDIR spectrum of the BWM cluster is shown in Figure 4b, flanked on either side by the corresponding pure BW_2 (Figure 4a) and BM_2 (Figure 4c) clusters for comparison. The inclusion of these spectra highlights trends that accompany the substitution of methanol for water in a single $n + m$ series (here $n + m = 2$). As expected, one

TABLE 4: Calculated OH Stretch Vibrational Frequencies and Infrared Intensities for Selected BW$_n$M$_m$ Structures[a,b]

structure/topology	frequency (cm^{-1})	frequency shift[c] (cm^{-1})	intensity (kM/mol)
BWM (A) chain	3552.3	−238.1	418.4
	3697.5	−92.9	233.8
	3817.5	27.1	79.2
BWM (B) chain	3596.5	−193.9	439.0
	3685.9	−104.5	146.6
	3819.6	29.2	137.1
BWM$_2$ (A) chain	3452.1	−338.3	654.4
	3505.4	−285.0	812.6
	3680.5	−109.9	298.0
	3813.7	23.3	66.8
BWM$_2$ (B) chain	3447.6	−342.8	874.1
	3529.3	−261.1	512.3
	3681.8	−108.6	298.7
	3807.2	16.8	85.9
BWM$_2$ (C) chain	3483.7	−306.7	676.9
	3533.5	−256.9	754.9
	3666.7	−123.7	215.2
	3813.9	23.5	129.0
BWM$_2$ (D) cycle	3459.5	−330.9	105.5
	3520.1	−270.3	741.8
	3544.8	−245.6	554.0
	3778.6	−11.8	140.1
BW$_2$M (A) cycle	3449.3	−341	86.7
	3502.5	−287.9	835.0
	3567.4	−223	363.0
	3779.1	−11.3	132.2
	3816.7	26.3	75.2
BW$_2$M (B) cycle	3432.1	−358.3	235.0
	3530.1	−260.3	399.0
	3554.4	−236	555.0
	3777.6	−12.8	138.0
	3819.2	28.8	75.9

[a] Calculations performed at the Becke3LYP/6-31+G(d) level of theory. [b] Calculated CH and OH stretch vibrational frequencies and infrared intensities for the W$_n$M$_m$ solvent clusters are available upon request. [c] Frequency shift relative to the average of the symmetric and antisymmetric stretches of the water monomer calculated at the same level of theory (3790.4 cm^{-1}).

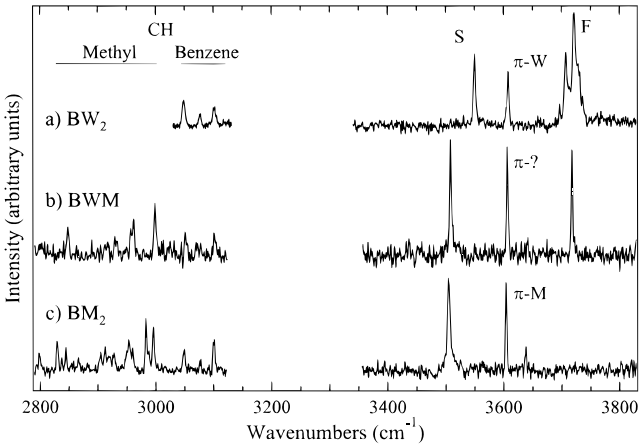

Figure 4. (a)−(c) Overview RIDIR spectra of BW$_n$M$_m$ clusters with $n + m = 2$. The R2PI transitions used to record the RIDIR spectra are labeled in Figure 2a,b). The OH stretch region stretches from 3500 to 3730 cm^{-1}. In the CH stretch region, transitions due to benzene appear in the 3050−3100 cm^{-1} region, while those due to the methyl CH stretches of methanol occur at 2800−3000 cm^{-1}.

OH stretch fundamental is lost from the spectrum upon each substitution of methanol for water in the $n + m = 2$ series, leading to four, three, and two OH stretch fundamentals in Figure 4−c, respectively. The frequencies of the OH stretch bands in BWM and the close correspondence of these bands to those in BW$_2$ and BM$_2$ point to a similar structure for BWM;

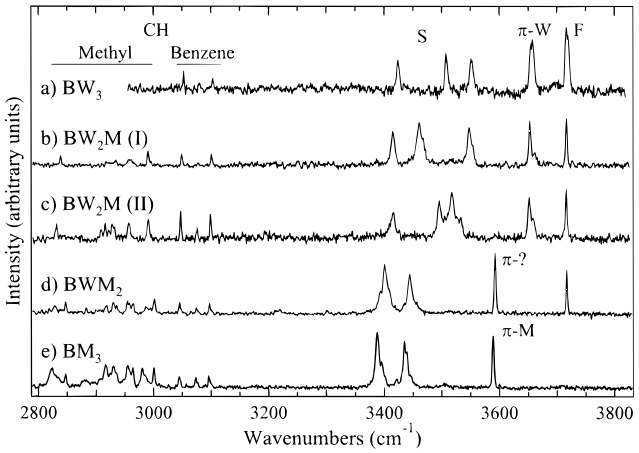

Figure 5. (a)−(e) Overview RIDIR spectra of BW$_n$M$_m$ clusters with $n + m = 3$. The R2PI transitions used to record the RIDIR spectra are labeled in Figure 2c,d). Characteristic absorptions due to free OH stretch (3710−3730 cm^{-1}), π H-bonded OH stretch (∼3650 cm^{-1}), single-donor OH stretch (3350−3550 cm^{-1}), benzene CH stretch (3050−3100 cm^{-1}), and methyl CH stretch (2800−3000 cm^{-1}) are apparent. The water-rich clusters of (a) to (c) are complexed to benzene through a W→B π H-bond. The methanol-rich clusters (d) to (e) are attached to benzene through a M→B π H-bond. See the text for further discussion.

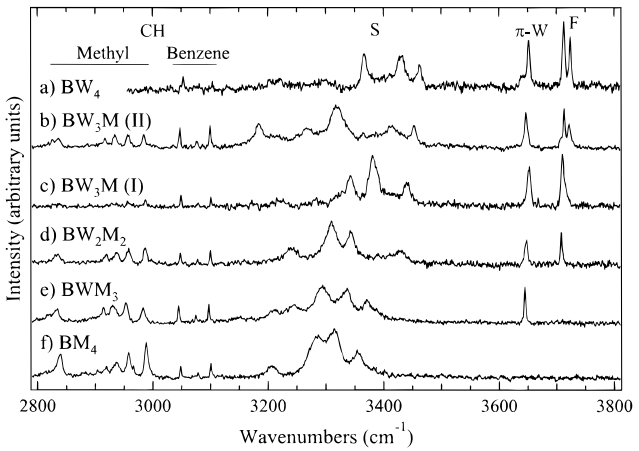

Figure 6. (a)−(f) Overview RIDIR spectra of BW$_n$M$_m$ with $n + m = 4$. The R2PI transitions used to record the RIDIR spectra are labeled in Figure 2d−g. Characteristic absorptions due to free OH stretch (3710−3730 cm^{-1}), π H-bonded OH stretch (∼3650 cm^{-1}), single-donor OH stretch (3150−3500 cm^{-1}), benzene CH stretch (3050−3100 cm^{-1}), and methyl CH stretch (2800−3000 cm^{-1}) are apparent. All solvent subclusters (with the exception of BM$_4$) are complexed to benzene through a W→B π H-bond. See the text for further discussion.

namely, one in which the acceptor molecule of a H-bonded WM dimer is involved in a π H-bond to benzene. Such a structure would produce a free OH, a π H-bonded OH, and a O−H···O H-bonded OH, as observed.

What is unclear from the OH stretch transitions is which substitutional isomer is present, B←M←W or B←W←M. To help distinguish between these possibilities, DFT Becke3LYP calculations were carried out on the two isomers. The structures of the two isomers (labeled A and B) are shown as insets in Figure 7a,b). The computed binding energies (Table 3) show a preference for structure A, in which methanol accepts a H-bond from water, over structure B, by 0.33 kcal/mol (after ZPE corrections). However, this energy difference is small enough that on this basis alone one cannot rule out either possibility.

Figure 7 compares the calculated infrared spectra for the two isomers with experiment. As in previous work,[30,32,33] the

TABLE 5: Experimental OH Stretch Frequencies, Frequency Shifts, and Assignments for BW_nM_m Clusters[a]

structure/ topology	BW_nM_m ν	$\Delta\nu^b$	width	OH assignment	structure/ topology	BW_nM_m ν	$\Delta\nu^b$	width	OH assignment
BWM chain	3508	−198	(3)	W-M H-bond	BW_3M(II) cycle	3184	−522.5	(21)	
	3606	−100	(3)	M πH-bond		3267	−439.5	(26)	
	3718	12	(<3)	W Free OH		3317	−389.5	(30)	
BWM_2 chain	3401	−305	(10)			3414	−292.5	*c*	
	3444	−262	(9)			3453	−253.5	(11)	
	3592	−114	(3)	M πH-bond		3647	−59.5	(6)	W πH-bond
	3717	11	(<3)	W Free OH		3713	6.5	(4)	W Free OH
BW_2M(I) cycle	3415	−291	(8)			3722	15.5	(7)	W Free OH
	3461	−245	(14)						
	3547	−159	(9)		BW_2M_2 cycle	3242	−465	(28)	
	3653	−53	(5)	W πH-bond		3310	−397	(27)	
	3717	11	(4)	W Free OH		3342	−365	(20)	
BW_2M(II) cycle	3416	−290	(8)			3429	−278	*c*	
	3495	−211	(9)			3648	−58	(6)	W πH-bond
	3517	−189	(11)			3708	2	(4)	W Free OH
	3651	−55	(6)	W πH-bond					
	3716	10	(3)	W Free OH	BWM_3 cycle	3211	−495	*c*	
BW_3M(I) cycle	3342	−364	(16)			3245	−461	*c*	
	3381	−325	(20)			3294	−412	(35)	
	3441	−265	(14)			3337	−369	(30)	
	3653	−53	(7)	W πH-bond		3370	−336	*c*	
	3710	4	(6)	W Free OH		3645	−61	(4)	W πH-bond

[a] All experimental frequencies, shifts, and widths (FWHM) reported in wavenumbers (cm^{-1}). [b] Frequency shifts reported with respect to the average of the symmetric and antisymmetric stretches of the water monomer (3706.5 cm^{-1}). [c] Unresolved transitions.

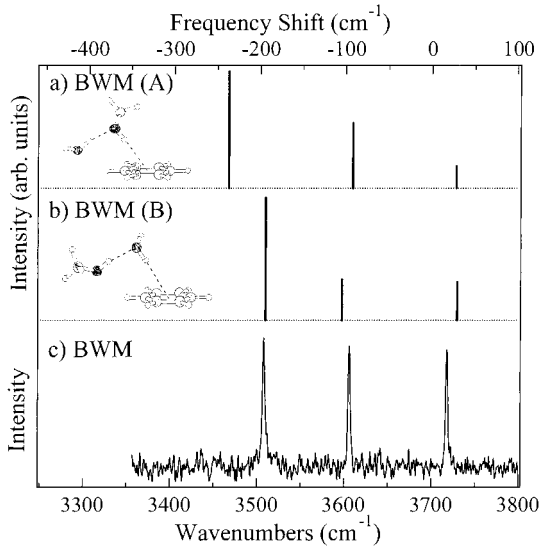

Figure 7. (a) and (b) Calculated OH stretch vibrational frequencies and infrared intensities for the two substitutional isomers of BWM (A and B) using DFT Becke3LYP with a 6-31+G(d) basis set. The zero of the frequency shift scale is set at the mean of the symmetric and antisymmetric stretch frequencies of water monomer at the same level of theory (3790.4 cm^{-1}). (c) Experimental RIDIR spectrum of BWM. The calculations cannot distinguish between the isomers based on the OH stretch region. See the text for further discussion.

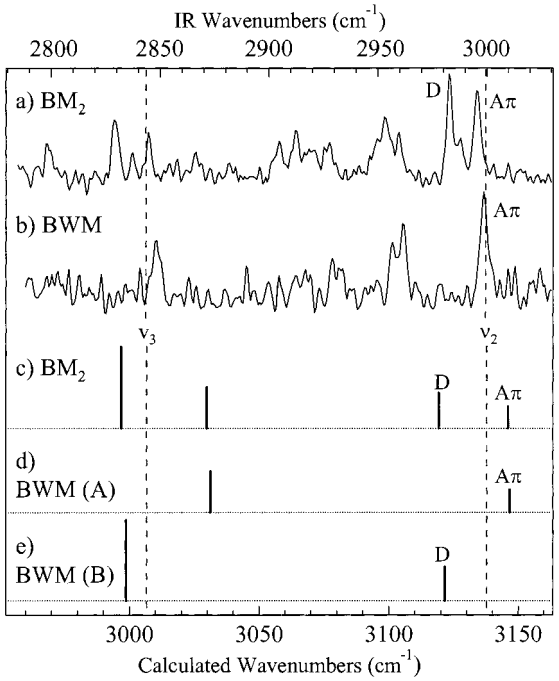

Figure 8. (a) and (b) RIDIR spectra of BM_2 and BWM in the methyl CH stretch region. The positions of the three CH stretch fundamentals (ν_2 and ν_3) in the methanol monomer are given by the vertical dotted lines. The labels on the ν_2 absorptions indicate the type of methanol (OH···O donor = D and OH···O acceptor/π donor = Aπ), as indicated in the insets. The donor CH stretch absorption is missing from the BWM spectrum, indicating that the BWM isomer observed experimentally is BWM (A) (see Figure 7a), in which methanol is in the Aπ position.

comparison is made by means of the vibrational wavenumber shift using the mean of the symmetric and antisymmetric stretch modes of water (3790.4 cm^{-1}), calculated at the same level of theory, as the zero of the relative wavenumber scale. The good correspondence with experiment confirms the general H-bonding topology of the BWM clusters as composed of a WM dimer that is π H-bonded to benzene. However, the similarity of the computed spectra for isomers A and B makes it difficult on this basis to distinguish which is found experimentally.

As discussed in the preceding article,[36] methanol's methyl CH stretch region offers an alternative probe of the local H-bonding environment of the methanol in the cluster. The present case is an ideal one to test the usefulness of the CH stretch region for this purpose, since the methanol molecule is a H-bond donor (D) in isomer B and an O−H···O acceptor/π donor (Aπ) in isomer A. Parts a and b of Figure 8 present closeups of the methyl CH stretch region of BM_2 and BWM, respectively. The former cluster serves as a useful comparison since it possesses both D and Aπ methanols. If the assignments of the bands in BM_2 are accepted, the presence of the bands

assigned to the Aπ methanol in BWM makes it clear that it is isomer A, and not B, that is experimentally observed.

The computed spectra of isomers A and B in Figure 8d,e confirm this assignment. The stick diagrams include only the ν_2 and ν_3 modes at the high- and low-frequency end of the spectra, since these are removed from the congested region due to the CH bend overtones and combination bands in the 2900−2950 cm^{-1} region. The ν_2 and ν_3 harmonic frequencies are shifted to characteristic positions depending on whether the methanol is a donor or acceptor/π molecule.

2. BW$_n$M$_m$ with $n + m = 3$. The RIDIR spectra of BW$_n$M$_m$ clusters with $n + m = 3$ (Figure 5) have characteristic OH stretch absorptions which depend on whether they are water-rich (BW$_3$ and BW$_2$M) or methanol-rich (BWM$_2$ and BM$_3$). This is the same division that was noted in earlier work based on vibronic level arguments from the R2PI spectra of the clusters.[29]

The series presented in Figure 5 shows the expected decrease in number of OH stretch transitions with increasing methanol content in the cluster. The RIDIR spectrum of BW$_3$ (Figure 5a) is that of a H-bonded W$_3$ cycle in which one of the free OH groups is π H-bonded to benzene.[44] This structure gives rise to six OH stretch fundamentals consisting of two free OH (unresolved at 3716 cm^{-1}), a π H-bonded OH (3657 cm^{-1}), and three single-donor OH groups in the H-bonded W$_3$ cycle. In the presence of benzene, the single-donor modes that are delocalized over the cycle in W$_3$, become partially localized in the presence of benzene, turning on intensity in the lowest-frequency in-phase stretching mode, and splitting the degeneracy of the higher frequency modes (Figure 5a).[44,53]

The other reference spectrum in the $n + m = 3$ series is that due to BM$_3$ (Figure 5e).[34,35] The three OH stretch fundamentals expected for this cluster are indeed observed but are not all single-donor transitions, as one would anticipate if the cyclic structure were retained. Instead, the spectrum is that of a methanol trimer H-bonded chain in which the terminal acceptor methanol in the M$_3$ chain forms a π H-bond with benzene.[34,35] As pointed out previously,[34,35] the BM$_3$ cluster presents a case in which the presence of benzene has modified the lowest-energy structure taken up by the solvent from cyclic to chain.

(a) BWM$_2$. In BWM$_2$, a single isomer dominates the R2PI spectrum (Figure 2d), appearing at a relative frequency of +154 cm^{-1} in the BM$_2^+$ mass channel. The RIDIR spectrum of this isomer is presented in Figure 5d. The close similarity with the spectrum of BM$_3$ (Figure 5e) is immediately apparent, with a single new transition in the free OH stretch region accompanying substitution of water for methanol. The presence of both a free OH stretch and a π H-bonded OH stretch rules out a cyclic WM$_2$ subcluster in BWM$_2$. The alternative, a WM$_2$ H-bonded chain, is the same structure anticipated by our earlier R2PI study of the cluster.[29]

Three substitutional isomers (C, B, and A) of BWM$_2$(chain) could be formed, with the single water molecule at the Aπ, AD, or D positions in the chain, as shown in Figure 9c−e, respectively. DFT calculations of these three isomers predict a slight energetic preference (Table 3) for isomer A (15.48 kcal/mol binding energy, ZPE corrected) over B (15.21 kcal/mol) and C (15.12 kcal/mol). However, the small size of these differences warn against drawing structural conclusions on this basis. Furthermore, the OH stretch harmonic frequencies and infrared intensities for the three isomers (Figure 9c−e) do not resolve the question of which structural isomer is observed experimentally. The calculations predict a similar frequency shift

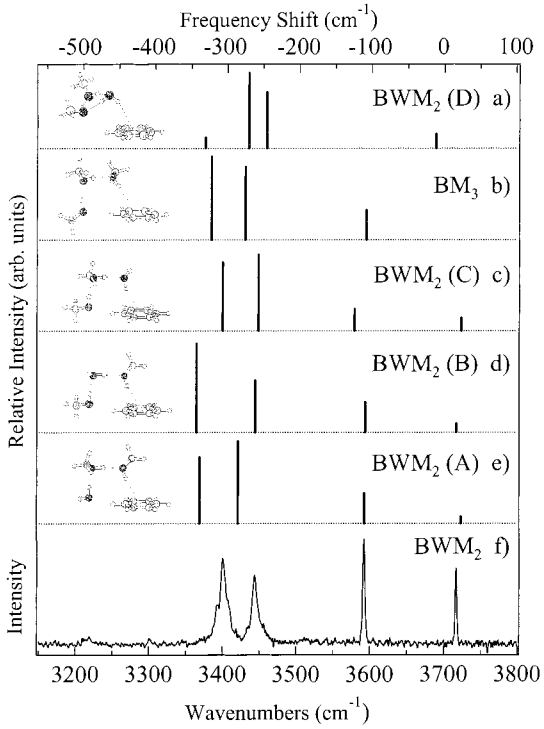

Figure 9. (a)−(e) Calculated OH stretch vibrational frequencies and infrared intensities for (a) BWM$_2$(cycle), (b) BM$_3$, and (c)−(e) three substitutional isomers of BWM$_2$(chain) using DFT Becke3LYP with a 6-31+G(d) basis set. The zero of the frequency shift scale is set at the mean of the symmetric and antisymmetric stretch frequencies of water monomer at the same level of theory (3790.4 cm^{-1}). (f) Experimental RIDIR spectrum of BWM$_2$. The calculations cannot distinguish between the isomers A−C based on the OH stretch region. See the text for further discussion.

for the π H-bonded OH stretch whether the π H-bond is formed with water or methanol.

To resolve this ambiguity, one looks to the methyl CH stretch region. Figure 10a juxtaposes the experimental RIDIR spectrum of BM$_3$ with that of BWM$_2$ (Figure 10b), where we have assigned[36] CH stretch absorptions to D, AD, and Aπ methanols in the M$_3$ chain (see the preceding paper). The ν_2 and ν_3 regions of the experimental spectrum of BWM$_2$ both contain an absorption ascribable to an acceptor/π methanol and a weaker transition in the frequency regime where one would anticipate an AD absorption. What is missing from the spectrum, by comparison to BM$_3$, is the donor CH stretch transition. One surmises on this basis that isomer A, in which water takes up a position as a terminal donor in the WM$_2$ chain, is that observed experimentally. This same conclusion is drawn from a comparison of the experimental with the computed spectra for the three isomers (Figure 10c−e). The methyl CH stretch modes show characteristic frequency shifts based on their position in the cluster. Only BWM$_2$(A) removes the donor methanol CH stretch modes from the spectrum, as observed experimentally.

It is interesting to note that the DFT Becke3LYP/6-31+G(d) calculations (Table 3) predict that the cyclic BWM$_2$ cluster is more strongly bound than chain BWM$_2$ by about 0.35 kcal/mol after zero-point energy correction. This is the opposite preference to that predicted by a semiempirical intermolecular potential in the earlier R2PI study of BW$_n$M$_m$ clusters.[29] Nevertheless, it is the chain BWM$_2$ cluster that is the dominant isomer observed in the experiment (Figure 2). One would anticipate that cyclic BWM$_2$, like its chain form, would appear almost exclusively in the BM$_2^+$ mass channel following loss of a single water molecule from the cluster during photoion-

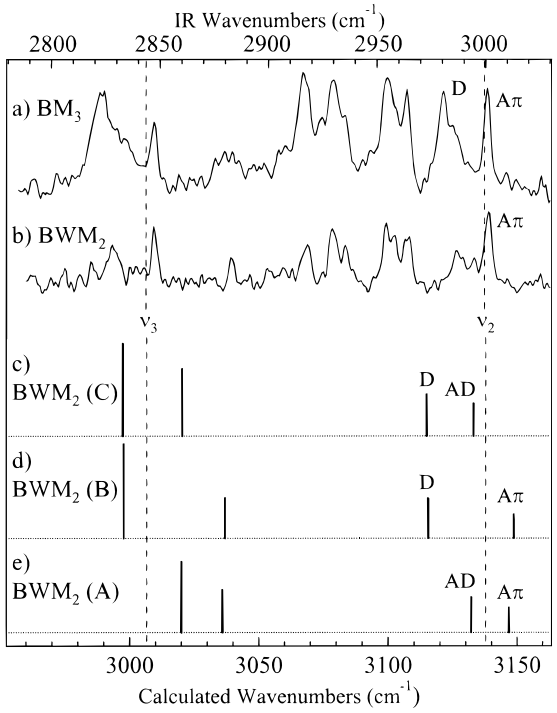

Figure 10. RIDIR spectra of (a) BM_3 and (b) BWM_2 in the methyl CH stretch region. The positions of the ν_1 and ν_3 CH stretch fundamentals in the methanol monomer are given by the vertical dotted lines. The labels on the ν_2 absorptions indicate the type of methanol (OH···O donor = D and OH···O acceptor/π donor = Aπ, and OH··· ·O acceptor/OH···O donor = AD), as indicated in the insets. The donor CH stretch absorption is missing from the BWM_2 spectrum, indicating that the BWM_2 isomer observed experimentally is BWM_2(A) (see Figure 9e), in which the water molecule takes up the acceptor position in the H-bonded chain.

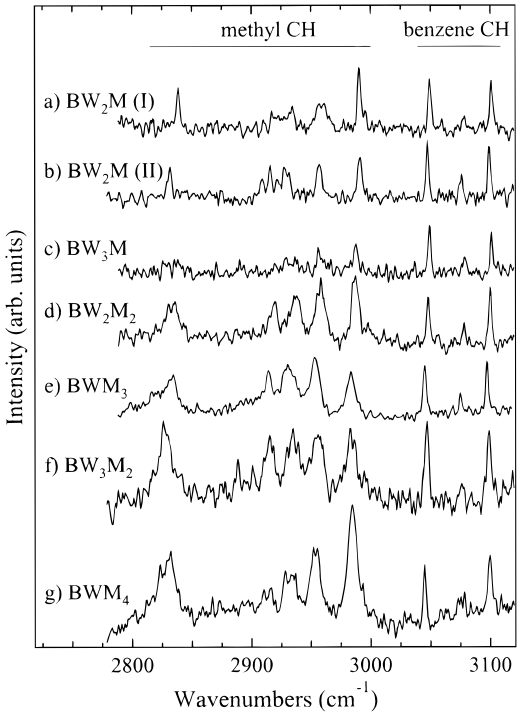

Figure 11. RIDIR spectra of the cyclic $n + m = 3$ [(a) BW_2M(I) and (b) BW_2M(II)], $n + m = 4$ [(c) BW_3M, (d) BW_2M_2, and (e) BWM_3], and $n + m = 5$ clusters [(f) BW_3M_2 and (g) BWM_4]. All the cyclic BW_nM_m clusters have methyl CH stretch spectra that are remarkably similar, reflecting the fact that all methanols in the cycles are AD methanols. The cyclic BW_4M spectrum is not included due to its marginal signal-to-noise.

ization. Two small peaks at +71 and +87 cm^{-1} are possible candidates for cyclic BWM_2 in the BM_2^+ mass channel, but their weak intensity has kept us from attempting to record RIDIR spectra of them. It seems likely that the experimental preference for chain over cyclic forms arises from the former having a larger binding energy. The present results have not included corrections for basis set superposition error, which could change the energy ordering between these two quite different H-bonding structures. Furthermore, the cyclic and chain BWM_2 clusters have quite different harmonic zero point energy corrections (Table 3), which could reverse the ordering if true anharmonic vibrational frequencies were used.

(b) The Two Cyclic Isomers of BW_2M. The RIDIR spectra of the two isomers of BW_2M both contain five OH stretch fundamentals (Figure 5b,c). The 3717 and 3716 cm^{-1} transitions in the spectra of BW_2M (I) and (II), respectively, are assigned to the free OH stretch of one of the water molecules in the clusters. The other transitions provide several pieces of evidence that both the observed isomers contain W_2M H-bonded cycles. First, the three transitions in the single-donor region can only be explained by a cyclic W_2M topology involving three O−H· ··O H-bonds. The spacing and intensity of these transitions differ between the two isomers, pointing out a means of distinguishing between them. Second, both BW_2M isomers also show transitions near the 3650 cm^{-1} region assignable to a W→B, rather than a M→B, π H-bonded OH group. A M→B π H-bond could not be formed while retaining the cyclic structure. Finally, the methyl CH stretch absorptions are characteristic of a cyclic H-bonding topology. As parts a and b of Figure 11 show, the BW_2M isomers have CH stretch spectra that bear a close resemblance to those of the other cyclic BW_nM_m clusters (Figure 11c−g). In cyclic W_nM_m structures, all methanol molecules are AD, producing particularly simple CH stretch spectra in which the transitions of all AD methanols in the cluster overlap to form three characteristic bands (due to ν_2, ν_3, and ν_9 modes of methanol) in the cluster spectrum.

Having determined that the two observed BW_2M isomers both contain cyclic W_2M subclusters, it remains to establish, if possible, the positions of the methanol molecule in the two isomers. In the absence of benzene, the W_2M cycle would have distinguishable isomers only in the out-of-plane positions of the methyl group and free water hydrogens in the cluster. This cyclic structure is the same one explored in some detail in the recent DFT calculations of Yanez and co-workers.[51] With benzene present, two structural isomers for BW_2M(cycle) can be formed, which differ in the position of the methanol molecule with respect to the π H-bound water, one donating to the π bound water in BW_2M(A) and another accepting a H-bond from it in BW_2M(B). Indeed, minima corresponding to these two structural isomers are located by the DFT calculations and are shown in Figure 12d,c, respectively. The figure also includes stick spectra of the OH stretch harmonic vibrational frequency shifts and infrared intensities for comparison with experiment. As Table 3 shows, the calculated structures differ in total binding energy (after zero-point energy corrections) by only 0.06 kcal/mol, with structure A more strongly bound than B in the absence of BSSE corrections.

Although the frequency shifts in the single-donor region are overestimated somewhat, the computed spectrum of BW_2M(B) (Figure 12c) shows a set of single-donor transitions with the same spacing and relative intensities to the experimental spectrum of BW_2M(II) (Figure 12f). Similarly, the BW_2M(A) stick diagram (Figure 12d) bears a distinct resemblance to the spectrum of BW_2M(I) (Figure 12e), though the relative intensi-

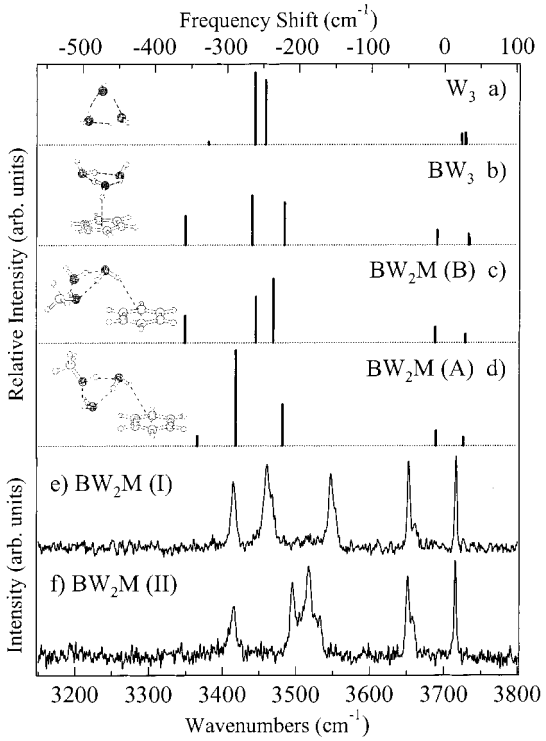

Figure 12. (a)−(e) Calculated OH stretch vibrational frequencies and infrared intensities for (a) W_3, (b) BW_3, and (c)−(d) two substitutional isomers of BW_2M(cycle) using DFT Becke3LYP with a 6-31+G(d) basis set. The zero of the frequency shift scale is set at the mean of the symmetric and antisymmetric stretch frequencies of the water monomer at the same level of theory (3790.4 cm^{-1}). (e)−(f) RIDIR spectra of BW_2M(I) and BW_2M(II) in the OH stretch region. The close correspondence between (c) and (f) leads to an assignment of BW_2M(II) as BW_2M(B), while that between (d) and (e) suggests that BW_2M(I) is BW_2M(A). See the text for further discussion.

ties are not perfectly matched. Saturation effects likely distort the experimental intensities to a certain degree. Despite this, the similarities between computed and experimental spectra are great enough to assign the spectrum of BW_2M(I) to isomer A (in which the methanol molecule acts as donor to the π bound water) and BW_2M(II) to isomer B (in which methanol is acceptor to the π bound water).

3. BW_nM_m with $n + m = 4$. The RIDIR spectra of BW_nM_m clusters with $n + m = 4$ (Figure 6b−e) are framed above and below by the corresponding spectra of BW_4 (Figure 6a) and BM_4 (Figure 6f) for comparison. A detailed analysis of these spectra will be taken up elsewhere.[22] For our purposes here, we need only note that all the spectra in this series are consistent with formation of cyclic W_nM_m subclusters, bound to benzene by a free OH on water, where possible. The CH stretch region of all the $n + m = 4$ clusters are consistent with their cyclic character (Figure 11c−e).

IV. Discussion

A. BW_nM_m Clusters and Preferential Solvation. The RIDIR spectra in the OH and CH stretch regions have provided the H-bonding topologies of several mixed BW_nM_m clusters with $n + m \leq 4$. These results, then, serve as a basis for assessing whether one of the solvents (water or methanol) preferentially binds to benzene in the clusters and how this preference changes with changing size and composition of the cluster. These are issues of preferential solvation.

A starting point for the discussion is provided by the mixed W_nM_m clusters without benzene present. The only experimental data available for mixed W_nM_m clusters is that for the WM mixed dimer, which is known from both microwave[24] and infrared spectroscopy[23,26] to be formed preferentially as the W→M isomer. This is also the prediction of the DFT calculations (Table 3), which show the W→M isomer to be more stable than M→W by 0.22 kcal/mol. This is consistent with methanol being a better H-bond acceptor than water due to electron donation from the methyl group onto methanol's accepting oxygen atom.

While no experimental data are available for larger W_nM_m clusters, the DFT calculations (Table 3) predict that the $n + m = 3$ and 4 clusters will preferentially form H-bonded cycles. As in the pure W_n and M_m clusters of this size, this configuration maximizes both the number of H-bonds in the cluster and the cooperative strengthening of these H-bonds.

When a benzene molecule is added to the cluster, it could change the W_nM_m structures preferred as a function of cluster composition and size. The H-bonded chains formed in BWM and BWM_2 place methanol at positions in the chain where it can accept an OH···O H-bond. Thus, the same W→M configuration preferred in the WM cluster is retained in BWM. Likewise, in BWM_2 the analogous W→M→M structure is preferentially formed. This configuration places methanol as terminal acceptor in the chain where it can π H-bond to benzene. Water is thus relegated to the exterior of these structures, with methanol preferentially solvating benzene.

In the $n + m = 3$ series, structures in which W_nM_m cluster is a H-bonded chain or cycle are close in energy to one another. A tradeoff occurs between forming three weaker, strained O−H···O H-bonds in the cycle and forming two, strong linear O−H···O H-bonds plus a cooperatively strengthened OH···π H-bond in the chain. The experimental finding is that the water-rich members of the series (BW_3 and the two observed isomers of BW_2M) clearly favor H-bonded cycles in that no R2PI transitions due to a chain species are observed. In the methanol-rich members (BWM_2 and BM_3), on the other hand, the H-bonded chain structure dominates. The most likely explanation for this structural rearrangement is that the chain structure has a greater total binding energy in the methanol-rich clusters, while the cycle does in the water-rich clusters.

In the $n + m = 4$ BW_nM_m clusters, cyclic W_nM_m subunits are preferentially formed in all cases, as anticipated on the basis of the cyclic structures found for BW_4 and BM_4. In the mixed clusters, the interaction with benzene is without exception via a π H-bond formed with a water OH not involved in the H-bonded cycle. Hence, unlike the H-bonded chains, when H-bonded cycles are formed, it is water that is preferentially bound to ("solvating") benzene, and methanol is relegated to positions further away.

In summary, the question of whether methanol or water preferentially solvates benzene in the BW_nM_m clusters is answered differently depending on the type of H-bonding structure taken up by the W_nM_m solvent subcluster. When the solvent forms a W_nM_m H-bonded chain, methanol preferentially binds to benzene, while a H-bonded W_nM_m cycle uses water to bind to benzene.

Since these conclusions are drawn from a study of cold, gas-phase BW_nM_m clusters, they probe the energetics of preferential solvation with the exclusion of entropic effects. Whether they will hold, even in bulk methanol/water solutions, is a subject for future experimental and theoretical work. The suggestion, based on energetics, is that local solvent environments that are H-bonded chains will tend to place methanol near benzene rather

than water. However, those that are cycles will prefer just the opposite circumstance.

B. OH Stretch IR Spectra and H-Bonding. Up to this point, the RIDIR spectra have been used mostly as a tool to determine the H-bonding topology of the BW_nM_m clusters. However, the correlation between the frequency shift of the OH stretch vibrations (relative to their value in the absence of a H-bond) and the strength of the H-bond enables us to extract from the spectra additional information about the relative strengths of the H-bonds formed between methanol, water, and benzene. The methanol monomer has an OH stretch fundamental at 3681 cm^{-1}, serving as the zero of the methanol frequency shift scale. In water, the average of the symmetric (3657 cm^{-1}) and antisymmetric stretch (3756 cm^{-1}) is used as the zero of the water OH relative frequency scale, thereby set at 3706 cm^{-1}. The frequency shifts of the OH stretch fundamentals in the $(n + m) = 2$ and $(n + m) = 3$ series provide quantitative evidence for the following conclusions:

1. The π H-bond formed to benzene by H-bonded chains is substantially stronger than that formed by H-bonded cycles.

2. Methanol's π H-bond to benzene increases in strength with the length of the chain but cares little for whether water or methanol is present elsewhere in the chain.

3. Methanol is a better H-bond acceptor than water, but water is the preferred donor.

The frequency shifts of the π H-bonded OH stretch fundamentals provide the evidence for points 1 and 2. However, one must be careful first to separate two effects. If the π-bound OH group is sufficiently isolated from other OH groups in the cluster, it produces a local mode OH stretch whose frequency directly reflects the strength of the π H-bond to benzene. On the other hand, if the π-bound OH is coupled to other OH groups in the cluster, it will be delocalized by that interaction and its frequency will depend in part on the strength of this OH−OH coupling. Of the observed clusters in the $(n + m) = 2$ and 3 series, only BW_2 has a π-bound molecule that has substantially delocalized OH stretch vibrations, with Aπ water OH stretch modes that are more nearly symmetric and antisymmetric stretch than free and π H-bonded OH stretches. In both BWM(A) and BM_2 clusters, the π-bound molecule is methanol and the π H-bonded OH stretch is a local mode. Relative to the OH stretch fundamental of the methanol monomer (3681 cm^{-1}), the π OH fundamentals of BWM(A) and BM_2 are shifted by −75 and −76 cm^{-1}, respectively. Upon addition of a third OH group to the chain, they are shifted still further to −89 and −92 cm^{-1} in BWM_2(A) and BM_3, respectively, approaching that of a M→M H-bond in methanol dimer ($\Delta\nu = -107$ cm^{-1}).[54]

By comparison, the π H-bonded OH stretch fundamentals formed by the H-bonded cycles in BW_2M (I and II) and BW_3 (Figure 5a−c) have far smaller frequency shifts of −53, −55, and −49 cm^{-1}, respectively, relative to the average of the symmetric and antisymmetric OH stretch modes of water (3706 cm^{-1}). In fact, for all BW_n clusters with $n = 1-9$ the π H-bonded OH stretch fundamentals have frequency shifts below −70 cm^{-1}, whether the W_n subclusters are cycles, cubes, expanded cubes, or other three-dimensional networks.[30,32,33,55] One surmises on this basis that the H-bonded chain is uniquely suited to forming a strong π H-bond to benzene and that this π H-bond undergoes significant cooperative strengthening as the length of the chain grows.

At the same time, the π-M OH stretch fundamentals in BWM(A) and BM_2 appear within one wavenumber of each other (−75 vs −76 cm^{-1}), showing little sensitivity to whether the π-bound methanol acts as H-bond acceptor to water or methanol. Similarly, in the BWM_2(A) and BM_3 clusters, the π H-bonded OH stretches are within 3 cm^{-1} of one another (Figure 5d,e), essentially unaffected by the change in water/methanol makeup of the chain.

For evidence supporting point 3, one can compare the single-donor OH stretch fundamentals of the BW_2, BM_2, and BWM(A) clusters. The single-donor OH stretch fundamentals are local mode OH stretch vibrations with frequency shifts of −156 cm^{-1} for W→W, −175 cm^{-1} for M→M, and −198 cm^{-1} for W→M in BW_2, BM_2, and BWM(A), respectively, indicating an ordering of H-bond strengths of (W→W) < (M→M) < (W→M). This is confirmed by the calculated structures (Table 2), which give O−O separations of 2.842 Å > 2.838 Å > 2.827 Å for the OH···O H-bonds in these three clusters. While the BWM(B) cluster is not observed experimentally, the prediction of the calculations is that the M→W H-bond is the weakest of the four W↔M possibilities, with an O−O separation of 2.852 Å.

C. Methyl CH Stretch Region. In the preceding paper[36] we established the frequency shift of methanol's methyl CH stretch fundamentals as a probe of the H-bonding environment of methanol, whether donor, acceptor, acceptor/donor, and the like. In the present work on mixed BW_nM_m clusters, the methyl CH stretch region has played a crucial role in our distinction between possible substitutional isomers. In the BWM and BWM_2 clusters, the OH stretch region established the existence of H-bonded chains, but it was the characteristic frequency shifts of the CH stretch transitions that were used to establish the positions of the methanol(s) in the chains. In the cyclic BW_nM_m clusters, the RIDIR spectrum in the CH stretch region confirmed their cyclic character even in cases where the OH stretch region was unusual in some way (e.g., BW_3M(II)).

These results, when combined with the results on methanol/acetone and methanol/water solutions reported in the preceding paper, provide some confidence that the CH stretch region can be used as a reliable probe of the H-bonding environment(s) of methanol under circumstances ranging from gas-phase clusters to the bulk.

Acknowledgment. We gratefully acknowledge NSF for support of this research under CHE-9728636. C.J.G. thanks Lubrizol Corp. for fellowship support.

References and Notes

(1) Reichardt, C. *Solvents and solvent effects in organic chemistry*; VCH: New York, 1988.

(2) Sadek, P. C. *The HPLC solvent guide*; John Wiley: New York, 1996.

(3) Rydberg, J.; Musikas, C.; Choppin, G. R. *Principles and practices of solvent extraction*; M. Dekker: New York, 1992.

(4) Franks, F.; Desnoyers, J. E. *Water Sci. Rev.* **1985**, *1*, 171−232.

(5) Williams, R. W.; Cheh, J. L.; Lowrey, A. H.; Weir, A. F. *J. Phys. Chem.* **1995**, *99*, 5299−5307.

(6) Onori, G. *Chem. Phys. Lett.* **1989**, *154*, 212−216.

(7) Crooks, J.; Stace, A. J.; Whitaker, B. J. *J. Phys. Chem.* **1988**, *92*, 3554−3560.

(8) Hester, R. E.; Plane, R. A. *Spectrochim. Acta* **1967**, *23A*, 2289−2296.

(9) Schwartz, M.; Moradi-Araghi, A.; Koehler, W. H. *J. Mol. Struct.* **1980**, *63*, 279−285.

(10) Kabisch, G.; Pollmer, K. *J. Mol. Struct.* **1982**, *81*, 35−50.

(11) Micali, N.; Trusso, S.; Vasi, C.; Blaudez, D.; Mallamace, F. *Phys. Rev. E* **1996**, *54*, 1720−1724.

(12) Soper, A. K.; Finney, J. L. *Phys. Rev. Lett.* **1993**, *71*, 4346−4349.

(13) Matsumoto, M.; Nishi, N.; Furusawa, T.; Saita, M.; Takamuku, T.; Yamagami, M.; Tamaguchi, T. *Bull. Chem. Soc. Jpn.* **1995**, *68*, 1775.

(14) Mizuno, K.; Miyashita, Y.; Shindo, Y.; Ogawa, H. *J. Phys. Chem.* **1995**, *99*, 3225−3228.

(15) Mashimo, S.; Umehara, T.; Redlin, H. *J. Chem. Phys.* **1991**, *95*, 6257−6260.

(16) Wakisaka, A.; Abdoul-Carime, H.; Yamamoto, Y.; Kiyozumi, Y. *J. Chem. Soc., Faraday Trans.* **1998**, *94*, 369−374.
(17) Guillaume, Y. C.; Guinchard, C. *Anal. Chem.* **1998**, *70*, 608−615.
(18) Liu, K.; Cruzan, J. D.; Saykally, R. J. *Science* **1995**, *271*, 929−33.
(19) Buck, U.; Schmidt, B.; Siebers, J. G. *J. Chem. Phys.* **1993**, *99*, 9428−37.
(20) Buck, U.; Schmidt, B. *J. Chem. Phys.* **1993**, *98*, 9410−24.
(21) Huisken, F.; Kaloudis, M.; Koch, M.; Werhahn, O. *J. Chem. Phys.* **1996**, *105*, 8965−8968.
(22) Hagemeister, F. C.; Gruenloh, C. J.; Zwier, T. S. *Chem. Phys.* **1998**, *239*, 83−96.
(23) Huisken, F.; Stemmler, M. *Chem. Phys. Lett.* **1991**, *180*, 332−338.
(24) Stockman, P. A.; Blake, G. A.; Lovas, F. J.; Suenram, R. D. *J. Chem. Phys.* **1997**, *107*, 3782.
(25) Bakkas, N.; Bouteiller, Y.; Loutellier, A.; Perchard, J. P.; Racine, S. *J. Chem. Phys.* **1993**, *99*, 3335.
(26) Bakkas, N.; Bouteiller, Y.; Loutellier, A.; Perchard, J. P.; Racine, S. *Chem. Phys. Lett.* **1995**, *232*, 90.
(27) Ben-Naim, A. *Preferential solvation in two- and in three-component systems*; Blackwell: Oxford, U.K., 1990; Vol. 62.
(28) Herrmann, C. U.; Wurz, U.; Kahlweit, M. *Ber. Bunsen-Ges. Phys. Chem.* **1978**, *82*, 560−67.
(29) Garrett, A. W.; Zwier, T. S.; Severance, D. L. *J. Phys. Chem.* **1992**, *96*, 9710−9718.
(30) Pribble, R. N.; Zwier, T. S. *Science* **1994**, *265*, 75−79.
(31) Pribble, R. N.; Zwier, T. S. *Faraday Discuss.* **1994**, *97*, 229.
(32) Gruenloh, C. J.; Carney, J. R.; Arrington, C. A.; Zwier, T. S.; Fredericks, S. Y.; Jordan, K. D. *Science* **1997**, *276*, 1678−1681.
(33) Gruenloh, C. J.; Carney, J. R.; Hagemeister, F. C.; Arrington, C. A.; Zwier, T. S.; Fredericks, S. Y.; Wood, J. T.; Jordan, K. D. *J. Chem. Phys.* **1998**, *109*, 6601−6614.
(34) Pribble, R. N.; Hagemeister, F.; Zwier, T. S. *J. Chem. Phys.* **1997**, *106*, 2145−2157.
(35) Hagemeister, F. C.; Gruenloh, C. J.; Zwier, T. S. *J. Phys. Chem. A* **1998**, *102*, 82−94.
(36) Gruenloh, C. J.; Florio, G. M.; Carney, J. R.; Hagemeister, F. C.; Zwier, T. S. *J. Phys. Chem. A* **1999**, *103*, 496.
(37) Pribble, R. N.; Gruenloh, C.; Zwier, T. S. *Chem. Phys. Lett.* **1996**, *262*, 627−632.
(38) Frisch, M. J.; Trucks, G. W.; Schlegel, H. B.; Gill, P. M. W.; Johnson, B. G.; Robb, M. A.; Cheeseman, J. R.; Keith, T. A.; Petersson, G. A.; Montgomery, J. A.; Raghavachari, K.; Al-Laham, M. A.; Zakrzewski, V. G.; Ortiz, J. V.; Foresman, J. B.; Peng, C. Y.; Ayala, P. Y.; Chen, W.; Wong, M. W.; Andres, J. L.; Replogle, E. S.; Gomperts, R.; Martin, R. L.; Fox, D. J.; Binkley, J. S.; Defrees, D. J.; Baker, J.; Stewart, J. P.; Head-Gordon, M.; Gonzalez, C.; Pople, J. A. *Gaussian 94 (Revision B.3)*; Gaussian, Inc.: Pittsburgh, PA, 1995.
(39) Clark, T.; Chandrasekhar, J.; Spitznagel, G. W.; v. R. Schleyer, P. *J. Comput. Chem.* **1983**, *4*, 294.
(40) Hehre, W. J.; Ditchfield, R.; Pople, J. A. *J. Chem. Phys.* **1972**, *56*, 2257.
(41) Becke, A. D. *J. Chem. Phys.* **1993**, *98*, 5648.
(42) Vosko, S. H.; Wilk, L.; Nusir, M. *Can. J. Phys.* **1980**, *58*, 1200.
(43) Lee, C.; Yang, W.; Parr, R. G. *Phys. Rev. B* **1988**, *37*, 785.
(44) Fredericks, S. Y.; Jordan, K. D.; Zwier, T. S. *J. Phys. Chem.* **1996**, *100*, 7810−7821.
(45) Fredericks, S. Y.; Pedulla, J. M.; Jordan, K. D.; Zwier, T. S. *Theor. Chem. Acc.* **1997**, *96*, 51−55.
(46) Kim, K.; Jordan, K. D.; Zwier, T. S. *J. Am. Chem. Soc.* **1994**, *116*, 11568−11569.
(47) Gotch, A. J.; Zwier, T. S. *J. Chem. Phys.* **1992**, *96*, 3388−3401.
(48) Garrett, A. W.; Zwier, T. S. *J. Chem. Phys.* **1992**, *96*, 3402−3410.
(49) Garrett, A. W.; Severance, D. L.; Zwier, T. S. *J. Chem. Phys.* **1992**, *96*, 7245−7258.
(50) Gotch, A. J.; Zwier, T. S. *J. Chem. Phys.* **1990**, *93*, 6977−86.
(51) Gonzalez, L.; Mo, O.; Yanez, M. *J. Chem. Phys.* **1998**, *109*, 139−150.
(52) The full set of vibrational frequencies is available from the authors upon request.
(53) Honegger, E.; Leutwyler, S. *J. Chem. Phys.* **1988**, *88*, 2582−95.
(54) Huisken, F.; Kulcke, A.; Laush, C.; Lisy, J. M. *J. Chem. Phys.* **1991**, *95*, 3924−3929.
(55) Pribble, R. N.; Garrett, A. W.; Haber, K.; Zwier, T. S. *J. Chem. Phys.* **1995**, *103*, 531−544.